EASR

Engineering and Applied Science Research

https://www.tci-thaijo.org/index.php/easr/index

Published by the Faculty of Engineering, Khon Kaen University, Thailand

Mathematical analysis of scaled-size clinker bed for temperature and pressure drop evaluation

Emmanuel Toluwalope Idowu*[1, 2)], Mutalubi Aremu Akintunde[2)], Taye Stephen Mogaji[2)], Olurotimi Akintunde Dahunsi[2)] and Sunday Joseph Oyepata[3)]

[1)]Department of Mechanical Engineering, Ajayi Crowther University, Oyo, Oyo State, Nigeria
[2)]Department of Mechanical Engineering, Federal University of Technology, Akure, Ondo State, Nigeria
[3)]BUA Cement Company (BUA International), Okpella, Edo State, Nigeria

Received 16 January 2024
Revised 6 July 2024
Accepted 17 July 2024

Abstract

In order to leverage on existing scaling methodologies, clinker bed was investigated to evaluate its performance for scaled down sizes. Small-sized clinker bed will provide cheaper and faster means of carrying out performance optimization study of clinker cooling process, which has been a research focus in recent years. Heat transfer mathematical equations were adopted to determine the outlet's temperatures and air pressure drop across the clinker bed, while Buckingham Pi theorem was employed to perform the scaling down of the clinker bed. Findings from the study revealed that for the actual size, predicted air outlet temperature, when compared to the experimental and numerical simulation results from existing literature, produced deviation of –5.46% and +1.65% respectively. For the scaled down-sizes, the air outlet temperature when compared with the actual size of experimental result, yielded deviations of 3.96%, 5.77% and 4.9% because the scaled sizes have 3, 6 and 9 scale factors, respectively. The results further revealed that an increase in mass flow rate of air will improve the heat transfer performance of the clinker bed, but this comes with an increase in pressure drop across the clinker bed heights. Furthermore, an increase in clinker flow rate was observed to be undesirable because the clinker outlet temperature actually being expected to cool down eventually increases, although pressure drop remained unchanged. By adopting a thermal-hydraulic performance factor (ϑ), maximum percentage deviation between ϑ of the actual size and each scaled size was 0.08% which indicates negligible performance deviation. The study therefore reveals that the size of clinker bed can be reduced to enable the development of small-scale prototype, and for numerical simulation to optimize the cooling process, especially when the outlet temperature and air pressure drop are the primary targets of investigation.

Keywords: Scaling, Temperature, Pressure drop, Clinker cooler, Porous media, Performance factor

1. Introduction

Heat transfer is primarily required to offset heat from high-temperature solid materials. These high-temperature solid materials are common intermediate products e.g. ceramic granules and cement clinkers, which needs to be cooled down for further processing or transportation [1]. Energy utilization in the global cement industry accounts for about 40 to 60% of the production cost [2], and the cement being the final product is the most manufactured product on earth [3]. Clinker is the fundamental component of the cement, produced through a baking process in a kiln and a subsequent cooling process in a clinker cooler [4]. Clinker coolers are important equipment in cement industry that recover heat from the hot clinkers by passing cooling air through the grate plates of the grate cooler upward through the pore space of the clinker bed [5, 6], thereby cooling down the hot clinker to a non-destructible temperature. Numerous studies have been carried out in order to improve the performance of clinker coolers. For instance, numerical simulation of heat transfer process in cement grate cooler was carried out by Shao et al., [7], using Fluent dynamic mesh technique and porous media model. From the study, the heat recovery boiler increases by 29.04°C and the ratio of heat effective utilization increases by 5.3%. Shao et al. [8] considered a multi-objective optimization of cooling air distributions of grate cooler with different clinker particle diameters and air chambers by genetic algorithm. The results show that the most effective and economic average diameter of clinker particles is 0.02 m. A theoretical study was performed for a coupled gas–solid heat transfer process in a moving cooling packed clinker bed by Cui et al. [9]. The study revealed that for the same clinker mass flow rate, operating with a thicker clinker layer can improve heat recovery and decrease the clinker outlet temperature. The distribution of heat transfer rates in the cement grate cooler shows that the first stage, the next four stages, and the last four stages undertake 47.87%, 48.49%, and 3.93% of the total heat load, respectively. In another study, experimental and numerical simulation of clinker cooling process was carried out by Shao et al. [10]. It was reported by the study that sensible heats of secondary and tertiary air, air discharge, clinker discharge, and the surface dissipation heat account for 50%, 40%, 9%, and 1% of the total heat flowing in the system, respectively. In a study by Wang et al. [11], numerical simulation and analytical characterization was carried out for unsteady heat transfer between cement clinker and air in a grate cooler. The model was developed using seepage heat transfer theory in porous media. The model analyzed the influence of grate speed and wind pressure on clinker cooling. Results from the study revealed that air temperature and clinker temperature increased with grate speed and decreased

*Corresponding author.
Email address: eidowu21@yahoo.com
doi: 10.14456/easr.2024.54

with air supply pressure. Another study by Wang et al. [12] further investigated heat transfer between clinker and cooling air with variable properties of grate cooler using the seepage approach. A seepage heat transfer model was constructed for compressible fluid flowing through a porous clinker layer, considering local thermal non-equilibrium and thermal dispersion effects. A solution algorithm for thermally coupled seepage was proposed. Simulation results showed a large deviation between the variable properties model and constant properties model, suggesting the variable properties model provides a more accurate description of clinker layer temperature distribution. In another study by Yao et al. [13], thermal efficiency model of the whole clinker calcination system was established by mass/heat balance analysis of its subunits, and its application was carried out on one 5000 MT/D production line. Findings from the study revealed that the thermal efficiency of the whole system is linearly correlated with the thermal efficiencies of its subunits. Increases in the thermal efficiency of each subunit lead to increases in the thermal efficiency of the whole system. As pointed out by Abdul et al. [14], research into thermodynamic modeling allows for product and process optimization of cement clinkers. However, considering the magnitude and chemistry of clinker production, there is a great challenge in modeling such a complex system. Hence, they developed a thermodynamic database with a specific application of cement clinkers. The developed model's effectiveness was shown through the prediction of real clinker, resulting to a good prediction for the main clinker phase compared against the experimental values. The results were favourable against the more traditional calculation methods. Okoji et al. [15] also studied the thermodynamic efficiency of a cement grate clinker cooling process. However, the study adopted the use of artificial neural network (ANN) and adaptive neural inference systems (ANFIS). The ANFIS optimal solutions are used to choose and validate the ultimate ideal kiln clinker discharge temperature, clinker mass flow, clinker cooling air, and ambient air. There is a notable reduction in energy usage when the ex-clinker cooler discharge temperature drops to 120 ℃, the energetic efficiency rises by 0.5%, and the total clinker cooling air lowers by 5% when compared to actual operational data.

In industrial applications where very large-sized equipment are used, for example, the clinker cooler in cement plants, a reliable scaling down is required to reduce the size of the clinker cooler or clinker porous bed to give a replica of the real size of the clinker bed that can be modeled easily. The reduction in size can be achieved through similarity theory. Similarity (Similitude) theory refers to the theory and art of predicting prototype conditions from model observations, by prescribing the relationship between full scale flow and a flow involving smaller but geometrically similar boundaries [16]. Coutinho et al. [17] defined similitude theory as a branch of engineering science concerned with establishing the necessary and sufficient conditions of similarity among phenomena. Similarity helps engineers and scientists to accurately predict the behavior of prototypes, through scaling laws applied to the experimental results of a scale model related to the prototype by similarity conditions [17, 18]. In designing and producing a prototype model based on a small-scale model, the prototype model is designed based on the similarity law, which establishes dimensionless factors for geometric shape, properties and flow characteristics between prototype and small-scale models [19]. Dimensional analysis offers identification of groups of variables whose interrelationships may be determined experimentally [20]. It is the basis of similarity theorem and is preferred because it is simple and fast to apply in problems where equations and boundary conditions cannot be fully expressed and not always helpful [21, 22]. In recent years, to overcome the obstacles associated with full-scale testing, such as cost and setup, research on similitude methods expanded into many branches of engineering [21]. Zhang et al. [23] performed experimental and numerical investigation on temperature profile of underground soil in the process of heat storage. Similarity conditions were derived, and a laboratory scaled-down thermal energy storage experiment model was developed. As reported by Zhou and Li [24], direct use of governing equations and dimensional analysis can be used to determine scale factors for scale model development of cylindrical shells and other structures. In a study by Fallico et al. [25], the influence of porous media typology on the scaling laws of confined aquifer characteristic parameters was investigated. Measurements were carried out on the confined aquifer, expressly reproduced in laboratory which allowed the determining of hydraulic conductivity values of performing a series of slug tests. Rushing into direct physical research is proven to be unproductive and uneconomical due to the physical size of clinker cooler units in cement plants. Better prospects are shown by an adequate scaling model in early research that may be further investigated by physical assessments. In a previous study by Oyepata et al. [26], a small-sized clinker cooler was developed to analyse the feasibility of modeling the performance of the clinker bed experimentally and through CFD. However, similarity procedure which enables modeling the clinker bed at varying sizes, taking into consideration different scaling factors was not evaluated. The use of scaling factors allows for modeling of the clinker bed at different sizes, while targeting achieving the same inlet and outlet temperature of clinker and air. Moreover, the cooling performance in terms of air pressure drop, pumping power and thermal-hydraulic performance factor were not considered. In addition, existing study on clinker cooler in literature did not provide adequate information to the best knowledge of the current authors. Hence, this study looks to extend the work carried out by Oyepata et al. [26], by adopting an analytical study on clinker cooling process using mathematical equations, taking into account the motion of a clinker bed. In view of this, similarity theory was adopted to scale down the size of the clinker bed to different sizes, while the performances of the beds were analyzed.

2. Methodology

Scaling the entire clinker cooler is robust and complex. A reliable approach is to focus only on the clinker bed and the operational parameters influencing the cooling process. Figure 1 shows a schematic description of 2D geometry of the porous clinker bed.

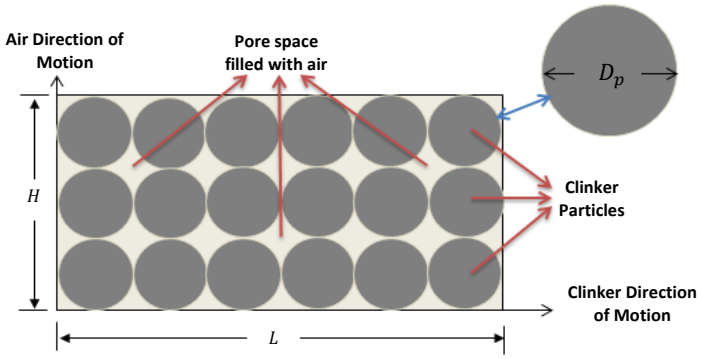

Figure 1 Schematic description of the 2D clinker porous bed

Data obtained from Cui et al. [9] which had been validated with experimental study, was adopted. The mathematical modeling of the grate clinker cooler considers the cooling to be in steady-state condition, with a cross flow heat exchange between hot clinker particles and cooling air mostly at ambient temperature. In modeling the cooling process, heat transfer and pressure drop are defined by mathematical equations [8, 27]. In order to achieve the development of the mathematical model, some assumptions were made. The assumptions are as follows [8, 27, 28]: clinker bed consists of homogenous spherical clinker particles; the temperature of hot clinker at rotary kiln exit is the same at cooler inlet; air flows vertically upwards through the clinker, quantities of fine particles transported by air flow are negligible and radiation heat transfer is not considered.

2.1 Mathematical study

Heat transfer rate between cooling air and clinker is given by equation (1) [8, 9, 29]:

$$Q = \Delta T_{diff} \times \frac{1-q}{1/C_{air} - [q/C_{clk}]} \quad (1)$$

where: term ΔT_{diff} is the difference between clinker inlet and air inlet temperatures, Q is the heat transfer rate (J/s) C_{clk} is the ratio of heat capacity rates of clinker (W/K) and C_{air} is the ratio of heat capacity rates of cooling air (W/K).

The term ΔT_{diff} is the difference between clinker and air inlet temperatures, estimated using equation (2):

$$\Delta T_{diff} = T_{clkin} - T_{airin} \quad (2)$$

The term C_{clk} in equation (1) is the ratio of heat capacity rates of clinker and is estimated using equation (3):

$$C_{clk} = \dot{m}_{clk} C_{pclk} \quad (3)$$

The velocity of clinker is estimated using equation (4):

$$U_{clk} = \frac{\dot{m}_{clk}}{HW\rho_{clk}} \quad (4)$$

The ratio of heat capacity rates of cooling air is estimated using equation (5):

$$C_{air} = \dot{m}_{air} C_{pair} \quad (5)$$

The superficial velocity of air is estimated from equation (6):

$$U_{air} = \frac{\dot{m}_{air}}{LW\rho_{air}} \quad (6)$$

The term q is estimated using equation (7):

$$q = exp\left(kA\left[\frac{C_{air}-C_{clk}}{C_{air}C_{clk}}\right]\right) \quad (7)$$

where: T_{clkin} is the temperature of clinker at inlet of the cooler (℃), T_{airin} is the temperature of air at inlet of the cooler (℃), ρ_{air} is the density of air (kgm^{-3}), $\dot{m}_{clk}$ is the mass flow rate of clinker (kg/s) and C_{pclk} is the specific heat capacity of clinker $(Jkg^{-1}K^{-1})$, U_{air} is the superficial velocity of air (m/s), U_{clk} is the velocity of clinker (m/s), L is the length of clinker bed (m), W is the width of clinker bed (m), C_{pair} is the specific heat capacity of clinker $(Jkg^{-1}K^{-1})$, k is the integrated heat transfer coefficient $(W/m^2/K)$ and A is the efficient heat transfer area (m^2)

The integrated heat transfer coefficient between cooling air and clinker, is given by equation (8) [1]:

$$k = \frac{1}{\frac{1}{h} + \frac{\varphi x}{\lambda_{clk}}} \quad (8)$$

Convective heat transfer coefficient between cooling air and clinker is given by equation (9) [8]:

$$h = \frac{Nu\lambda_{air}}{D_p} \quad (9)$$

Nusselt number is obtained using equation (10) [9, 29]:

$$Nu = 2 + 1.8Pr_{air}^{1/3} Re_{air}^{1/2} \quad (10)$$

Reynolds number of air is given by equation (11):

$$Re_{air} = \frac{\rho_{air} U_{air} D_p}{\mu_{air}} \quad (11)$$

Prandtl number of air is given by equation (12):

$$Pr_{air} = \frac{\mu_{air}\, C_{pair}}{\lambda_{air}} \tag{12}$$

where: h is convective heat transfer coefficient ($Wm^{-2}K^{-1}$), φ is the particle shape correction factor, taken to be 0.25 [1, 9], x is the clinker particle heating depth which is equal to the radius of clinker particle (m), λ_{clk} is the thermal conductivity of clinker particle ($Wm^{-1}K^{-1}$), μ_{air} is the kinematic viscosity of air ($kgm^{-1}s^{1}$), D_p is the average diameter of clinker particle (m), U_{air} is the superficial velocity of air (ms^{-1}) and λ_{air} is the thermal conductivity of air ($Wm^{-1}K^{-1}$) .

The effective heat transfer area between cooling air and clinker particle is given by equation (13):

$$A = \frac{6V_{clk}(1-\varepsilon)}{D_p} \tag{13}$$

The volume of clinker bed is equation (14):

$$V_{clk} = LWH \tag{14}$$

The clinker cooling process is simplified as a direct heat exchanger; hence the heat balance equation is applicable and expressed as [8, 30]:

$$C_{clk}(T_{clkin} - T_{clkout}) = Q = C_{air}(T_{airout} - T_{airin}) \tag{15}$$

Equation (15) can also be expressed as:

$$Q_{clk} = Q = Q_{air} \tag{16}$$

Clinker outlet temperature can be determined using equation (17):

$$T_{clkout} = T_{clkin} - \frac{Q_{clk}}{C_{clk}} \tag{17}$$

Air outlet temperature can be determined using equation (18):

$$T_{airout} = T_{airin} + \frac{Q_{air}}{C_{air}} \tag{18}$$

The pressure drop of cooling air across the bed is estimated using equation (19) [8, 29]:

$$\frac{\Delta P_{air}}{H} = \left[\frac{150\mu_{air}}{{D_p}^2} \times \frac{(1-\varepsilon)^2}{\varepsilon^3} \times U_{air}\right] + \left[\frac{1.75\rho_{air}}{D_p} \times \frac{1-\varepsilon}{\varepsilon^3} \times {U_{air}}^2\right] \tag{19}$$

where: ε is the porosity of the clinker bed, H is the height of clinker bed (m), ρ_{air} is the density of air (kgm^{-3}), ΔP_{air} is the pressure drop of cooling air (Pa), ε is the porosity, U_{air} is the superficial velocity of air (m/s).

The thermo-physical properties of air and clinker such as the density of air (ρ_{pair}), specific heat capacity of air (C_{pair}), specific heat capacity of clinker (C_{pclk}), thermal conductivity of air (λ_{air}), thermal conductivity of clinker (λ_{clk}) and dynamics viscosity of air (μ_{pair}) are based on fitting empirical equations (20), (21), (22), (23), (24) and (25), respectively [7, 31-33].

$$\rho_{pair} = (351.99/T_{air}) + (344.88/T_{air}^2) \tag{20}$$

$$C_{pair} = 955 + 0.14387T_{air} + 3.8525 \times 10^{-5}T_{air}^2 + 2.1036 \times 10^{-10}T_{air}^3 + 1.2052 \times \ 10^{-13}T_{air}^4 \ (Jkg^{-1}K^{-1}) \tag{21}$$

$$C_{pclk} = 699.5 + 0.31812T_{clk} - 6.2308 \times 10^{-5}T_{clk}^2 - 1.3753 \times 10^{-10}T_{clk}^3 - 5.1388 \times 10^{-14}T_{clk}^4 \ (Jkg^{-1}K^{-1}) \tag{22}$$

$$\lambda_{air} = 0.0244(T_{air}/273)^{0.759}(Wm^{-1}K^{-1}) \tag{23}$$

$$\lambda_{clk} = 0.244[1 + 0.00063(T_{clk} - 273)]\ (Wm^{-1}K^{-1}) \tag{24}$$

$$\mu_{pair} = 1.72 \times 10^{-5}[(273 + 114)/(T_{air} + 114)](T_{air}/273)^{1.5}\ (kgm^{-1}s^{-1}) \tag{25}$$

2.2 Scaling procedure

In this study, Dimensional Analysis Method was selected due to its simplicity and reliability [21]. Buckingham Pi theorem was used to establish the relationship between the variables that describe the clinker bed and the similarity conditions to be established between the real-size clinker bed and the scaled-down clinker bed. In order to determine the variables in the system, all the variables are listed and counted. The total number of variables is represented by V_n. The total number of variables is the sum of dependent

variables V_d and all the independent variables V_i. An expression for the temperature of clinker at the outlet of the clinker cooler after cooling (T_{clkout}) is determined. The variables used for the scaling are presented in Table 1. After a complete list of independent variables on the basis of correspondence of units is drawn up, and the selection of repeating variables completed, dimensionless pi (π**)** quantities are determined. In order to form the dimensionless pi groups, the repeating variables are combined with each of the other variables in turn. This implies that the Pi groups are formulated by multiplying each of the remaining variables that were not chosen as repeating variables in turn by the repeating variables, each in turn raised to some unknown exponent. The theory of similitude searches for a relationship which maps the scaling model's parameters onto the real-life size parameters. This means that each model parameter is proportional to its corresponding real size parameter. This proportional factor is called the scale factor [34].

3. Results and discussion

3.1 Scaled down parameters

From Table 1, there are ten (10) variables which were considered. The primary dimensions involved were also listed in the table and are a total of four (4) in number. The total number of dimensional variables is denoted by $V_n = 10$, the number of dependent variables is denoted by $V_d = 1$, the number of independent variables is denoted by $V_i = 9$ and the number of primary dimensions is denoted by $\mathrm{P}_r = 4$. The primary dimensions are Mass (M), Length (L), Temperature (θ) and Time (T). The number of reference dimensions is denoted by $V_i = 3$. They are (θ), (MT^{-1}) and (L). The required number of pi terms is estimated, and this is given by the difference between the total number of dimensional variables (V_n) and the total number of primary dimensions (P_r).

The dependent and independent variables are represented in the function below:

$$V_d = f(V_i) \tag{26}$$

$$T_{clkout} = f(T_{clkin},\ T_{airin},\ \dot{m}_{clk},\ \dot{m}_{air},\ D_p,\ W,\ H,\ L,\ \varepsilon) \tag{27}$$

The number of required pi terms is given by:

$$n_r = V_n - \mathrm{P}_r = 10 - 4 = 6 \tag{28}$$

Hence the number of required pi terms (n_r)= 6

Table 1 Scaling down variables

S/N	Symbol	Quantity	Unit	Dimensions	Variable Type
1	T_{clkout}	Clinker outlet temperature	℃	θ	Dependent
2	T_{clkin}	Clinker inlet temperature	℃	θ	Independent
3	T_{airin}	Air inlet temperature	℃	θ	Independent
4	$\dot{m}_{clk}$	Clinker inlet mass flow rate	kg/s	MT^{-1}	Independent
5	$\dot{m}_{air}$	Air inlet mass flow rate	kg/s	MT^{-1}	Independent
6	D_p	Average diameter of clinker	m	L	Independent
7	W	Width of clinker bed	m	L	Independent
8	H	Height of clinker bed	m	L	Independent
9	L	Length of clinker bed	m	L	Independent
10	ε	Porosity of the clinker bed	-	1 (Dimensionless)	Independent

Based on the rule of selecting repeating variables, dimensionless variables are automatically considered as a Pi group. Therefore, the total number of Pi term, is $n_t = 7$. The repeating variables selected, which satisfies the requirement for selection are: T_{clkin}, $\dot{m}_{clk}$ and L. In order to determine the Pi (π) groups, the function relating the dependent variable and independent variables is presented as:

$$T_{clkout} = f(T_{clkin},\ T_{airin},\ \dot{m}_{clk},\ \dot{m}_{air},\ D_p,\ W,\ H,\ L,\ \varepsilon) \tag{29}$$

Therefore, $\pi_1 = \frac{T_{clkout}}{T_{clkin}}$; $\pi_2 = \frac{T_{airin}}{T_{clkin}}$; $\pi_3 = \frac{\dot{m}_{air}}{\dot{m}_{clk}}$; $\pi_4 = \frac{D_p}{L}$; $\pi_4 = \frac{W}{L}$ and $\pi_6 = \frac{H}{L}$

The sixth Pi group, $\pi_7 = \varepsilon$. This is because the variable ε is already a dimensionless parameter and can be taken as a Pi group. The relation between the Pi (π) group as dimensionless parameters is presented as a function in the form:

$$\pi_1 = f(\pi_2,\ \pi_3,\ \pi_4,\ \pi_5,\ \pi_6,\ \pi_7) \tag{30}$$

Similarly,

$$\frac{T_{clkout}}{T_{clkin}} = f\left(\frac{T_{airin}}{T_{clkin}},\ \frac{\dot{m}_{air}}{\dot{m}_{clk}},\ \frac{D_p}{L},\ \frac{W}{L},\ \frac{H}{L},\ \varepsilon\right) \tag{31}$$

The next step as reported by Batul et al., [34] is to fix a number of factors, which is based on the number of repeating variables. Hence, three (3) factors were fixed, after which the scale factors for the other variable are determined, using the Pi products.

The scale factor value for temperature of clinker at inlet, $S_{fTClkin} = \frac{(T_{clkin})_{actual}}{(T_{clkin})_{scaled}} = 1$

The scale factor value for the length of the clinker bed, $S_{fL} = \frac{(L)_{actual}}{(L)_{scaled}} = 3$

The scale factor value for the mass flow rate of clinker, $S_{f\dot{m}_{clk}} = \frac{(\dot{m}_{clk})_{actual}}{(\dot{m}_{clk})_{scaled}} = 3$

The second step follows that Pi products of actual size and scaled size remain equal; therefore [34]:

for the first Pi group (π_1), $S_{fTClkout} = \frac{(T_{clkin})_{actual}}{(T_{clkin})_{scaled}} = \frac{(T_{clkout})_{actual}}{(T_{clkout})_{scaled}} = 1$; for the second Pi group (π_2), $S_{fTairin} = \frac{(T_{airin})_{actual}}{(T_{airin})_{scaled}} = \frac{(T_{clkin})_{actual}}{(T_{clkin})_{scaled}} = 1$; for the third Pi group (π_3), $S_{fTairin} = \frac{(\dot{m}_{air})_{actual}}{(\dot{m}_{air})_{scaled}} = \frac{(\dot{m}_{clk})_{actual}}{(\dot{m}_{clk})_{scaled}} = 3$, for the fourth Pi group (π_4), $S_{fD_p} = \frac{(D_p)_{actual}}{(D_p)_{scaled}} = \frac{(L)_{actual}}{(L)_{scaled}} = 3$, for the fifth Pi group (π_5), $S_{fW} = \frac{(W)_{actual}}{(W)_{scaled}} = \frac{(L)_{actual}}{(L)_{scaled}} = 3$; and for the sixth Pi group (π_6), $S_{fH} = \frac{(H)_{actual}}{(H)_{scaled}} = \frac{(L)_{actual}}{(L)_{scaled}} = 3$.

The seventh Pi group, $\pi_7 = \varepsilon$ is a dimensionless variable. In addition, the porosity of a clinker bed is expressed as the ratio of volume of pores space and the volume occupied by the particles.

3.2 Validation of mathematical study and scaled-down sizes

Table 2 presents the operational parameters of the actual size and scaled down clinker bed. The experimental data used for the validation of the mathematical equations are presented in Table 3. Figure 2 shows a schematic description of clinker cooling in a clinker cooler.

Table 2 Operating parameters of actual size and scaled down clinker bed

Parameter	Symbol	Unit	Scale factor		
Clinker inlet temperature	T_{clkin}	℃	1	1	1
Clinker outlet temperature	T_{clkout}	℃	1	1	1
Air inlet temperature	T_{airin}	℃	1	1	1
Clinker inlet mass flow rate	$\dot{m}_{clk}$	kg/s	3	6	9
Air inlet mass flow rate	$\dot{m}_{air}$	kg/s	3	6	9
Average diameter of clinker particle	D_p	m	3	6	9
Width of clinker bed	W	m	3	6	9
Height of clinker bed	H	m	3	6	9
Length of clinker bed	L	m	3	6	9
Porosity of the clinker bed	ε	-	1	1	1

Table 3 Clinker cooler data from cement plant

Parameter	Symbol	Unit	Cui *et al*. [9]
Clinker inlet temperature	T_{clkin}	℃	1365
Clinker outlet temperature	T_{clkout}	℃	-
Air inlet temperature	T_{airin}	℃	30
Air outlet temperature	T_{airout}	℃	1160.25
Clinker mass flow rate	$\dot{m}_{clk}$	kgs^{-1}	72.32
Air mass flow rate	$\dot{m}_{air}$	kgs^{-1}	35.17
Average diameter of clinker	D_p	m	0.04
Width of clinker bed	W	m	4.00
Height of clinker bed	H	m	0.75
Length of clinker bed	L	m	3.26
Porosity	ε	-	0.4

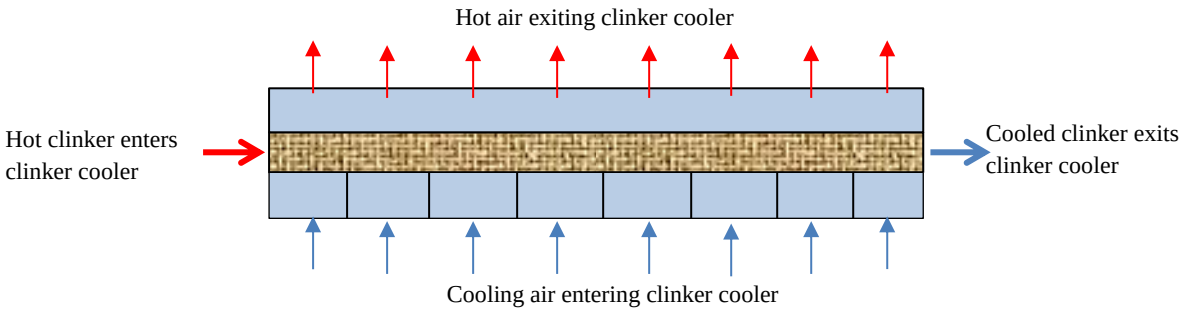

Figure 2 Simplified clinker cooling process in clinker coolers

The data obtained from [9] are for a cement plant with an overall length of clinker bed of 35.89 m. The heat exchange principle taking place between clinker and air is the same along the entire length of the clinker cooler. Therefore, each air chamber can be analyzed separately, which makes it easier to simplify the analysis by selecting only the first air chamber. Hence, the first air chamber

was selected for scaling down and verification was carried out. As reported in the works of [9] and [10], secondary air comes mainly from the outlet of first air chambers. Based on industrial measurements, the secondary air outlet temperature corresponding to the first air chamber is 1160.25 °C [9, 10], while the numerical simulation results estimated by Cui et al. [9] is 1079.06 °C. This represents a relative error of –7.0% which is within acceptable limit. The mathematical analysis carried out for this study, predicted air outlet temperature to be 1096.9 °C and when compared to the experimental and numerical simulation value of [9], the relative errors were –5.46% and +1.65% respectively. The direct and simplified mathematical equations were employed to verify the scaling down procedure by comparing the values of air outlet and clinker outlet temperatures, and air pressure drop for the scaling factors selected. The relative errors between the actual size clinker and air outlet temperatures and the scaled down outlet temperatures were also determined, using equation (32) and (33) for clinker and air respectively.

$$E_{rC} = \frac{T_{c.o.A} - T_{c.o.S}}{T_{c.o.A}} \times 100 \tag{32}$$

$$E_{rA} = \frac{T_{A.o.A} - T_{A.o.S}}{T_{A.o.A}} \times 100 \tag{33}$$

where: E_{rr} is the initial relative error, T_{Exp} is the experimental air outlet temperature, and $T_{N/M}$ is numerical or theoretical air outlet temperature. E_{rC} is the relative error for clinker, E_{rA} is the relative error for air, $T_{c.o.A}$ is actual size clinker outlet temperature, $T_{A.o.A}$, is the actual size air outlet temperature, $T_{c.o.S}$ is the scaled down size clinker outlet temperature, and $T_{A.o.S}$ is the scaled down size air outlet temperature.

For the scaled down clinker bed, when scale factor 3, 6 and 9 were considered, the estimated T_{airout} are 1114.3℃, 1093.3℃ and 1103.2℃ respectively, with relative errors of 3.96%, 5.77% and 4.9% respectively when compared to experimental value, 1160.25℃. Figure 3 shows a graphical comparison of the air outlet temperatures for experimental and numerical simulation obtained from [9], for actual size of clinker bed, and mathematical analysis in this study for scale factor 1 (actual size), 3, 6 and 9. In Figure 4, clinker and air outlet temperatures were compared for actual size, and scaled down sizes using scale factors 3, 6 and 9. The result of air outlet temperature in Figure 3 basically presents the comparison between literature (actual size only), and the different sizes (actual size and different scale factor) in the current study.

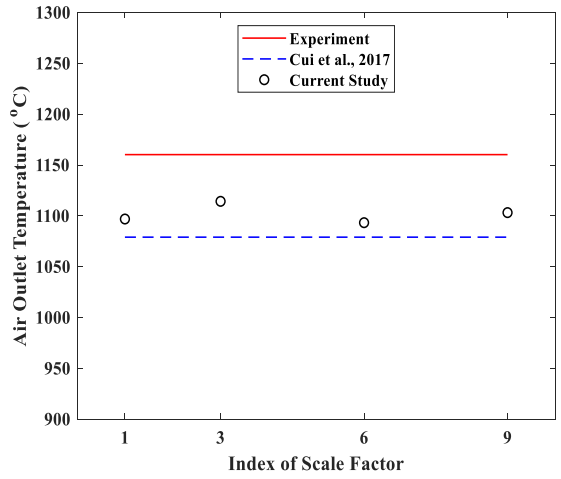

Figure 3 Comparison of air outlet temperatures; experiment, Cui *et al*. [9] and Current Study

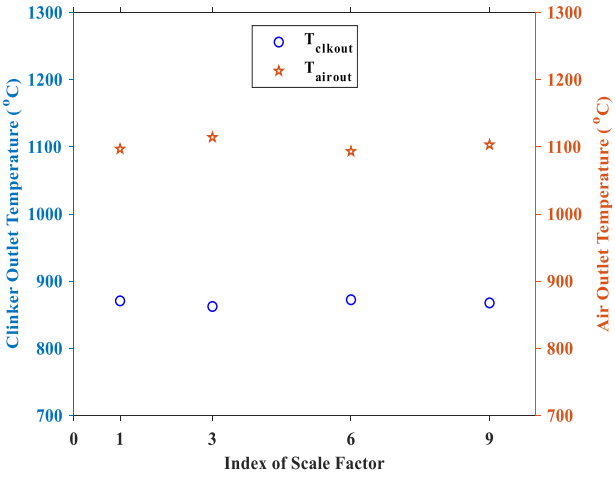

Figure 4 Comparison of estimated clinker and air outlet temperatures for different scaling factors

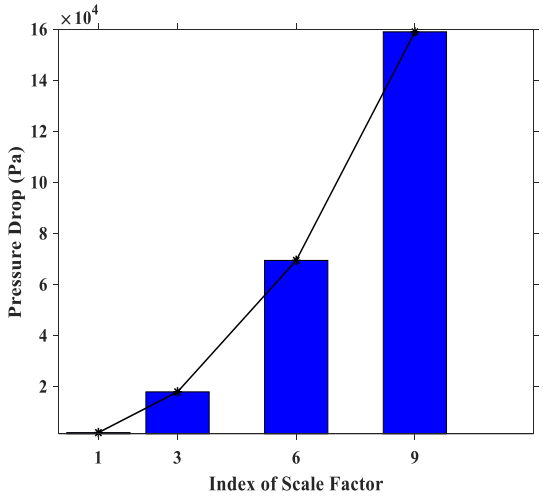

Figure 5 Comparison of estimated pressure drop for different scaling factors

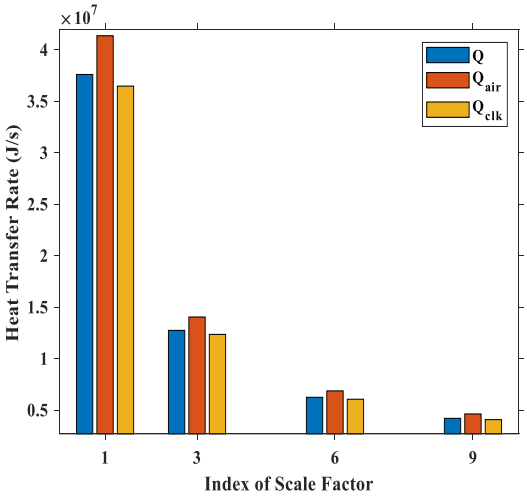

Figure 6 Comparison of heat transfer rate for different scaling factors

For instance, the straight continuous line represents air outlet temperature for experimental study at actual size, while the dotted line represents air outlet temperature for simulation study at actual size. The circular points represent the temperature of actual size (1) and the other three scale-down sizes with scale factors 3, 6, 9. The variations in the results are due to the approximation taken into account during computation and, hence, there is the need to compare the study to ascertain that the deviation are within acceptable range. The actual size of the clinker bed is represented by scale factor 1. From the mathematical analysis, clinker outlet temperature, T_{clkout} estimated for the actual size of the clinker bed is 870.7 ℃ . For the scaled down clinker bed, when scale factor 3, 6 and 9 were considered, the estimated T_{clkout} are 862.4℃, 872.4℃ and 867.7℃ respectively, with relative errors of 0.95%, 0.19% and 0.34% respectively. Similarly, air outlet temperature, T_{airout} estimated for the actual size of the clinker bed is1096.9 ℃ . It is important to note that the scaling factors for the inlet and outlet temperatures were assigned as "1" to ensure that the same initial temperature was maintained irrespective of the size of the clinker bed. Pressure drops were also compared as shown graphically in Figure 5. Pressure drop increases with increase in scale factor. The heat transfer rates values estimated were also considered and presented in Figure 6. For the actual size clinker bed, expected heat transfer rate (Q) estimated is 37602000 J/s, while the air heat transfer rate (Q_{air}) and clinker heat transfer rate (Q_{clk}) are 41367000 J/s and 36474000 J/s respectively. The deviation error between expected, and air and clinker heat transfer rate are + 9.1% and – 2.9% respectively. Similar deviation errors, estimated for scale factors 3, 6 and 9 give; + 10% and – 3.1%, + 9.9% and – 2.9%, and + 10% and – 3% respectively.

3.3 Effect of cooling air flow rate on outlet temperatures and air pressure drop

The performance of the clinker bed first air chamber (Actual size and scaled-down sizes) was investigated by varying the mass flow rate of the cooling air and was presented in Figure 7. Other inputs and geometrical parameters remain the same, while the cooling air mass flow rate is varied from 30 kg/s to 40 kg/s at intervals of 2 kg/s. As shown in Figure 7, the clinker outlet temperature decreases with increase in mass flow. This phenomenon was observed to maintain the same trend for all the sizes of clinker bed. Clinker bed with scale factor 6 predicted the maximum temperatures for each flow rate, with the values very close to the actual size clinker bed. Clinker bed with scale factor 3, on the other hand produces minimum temperature values for each flow rate. In general, the minimum temperature 826.45℃ was estimated at flow rate 40 kg/s (i.e. actual size) for scale factor 3, while the maximum temperature 916.57℃ was estimated at flow rate 30 kg/s (i.e. actual size) for scale factor 6. Figure 8 presents the variation of air mass flow rate with air outlet temperature. The performance evaluation shows that as air inlet flow rate increases, the outlet temperature of air decreases. Figure 9 shows variation of air inlet flow rate with difference between clinker outlet temperature and air outlet temperature for the actual size of the clinker bed. The performance show that as the clinker and air outlet temperatures decrease, with increase in air inlet flow rate, their corresponding difference also decreases. Figure 10 shows the variation of air inlet mass flow rate with clinker and air outlets temperature difference and pressure drop for the actual size. The variation revealed that as the air flow rate increases, the temperature difference decreases, while the pressure drop increases. Increase in pressure drop is considered unfavorable because it implies increase in pumping cost.

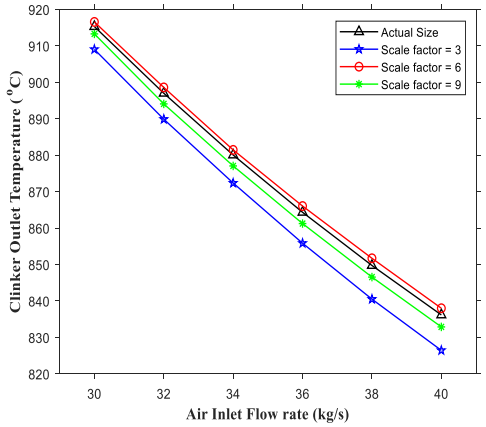

Figure 7 Variation of air inlet mass flow rate with clinker outlet temperature

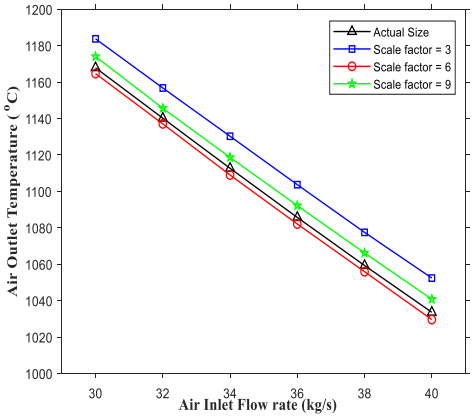

Figure 8 Variation of air mass flow rate with air outlet temperature

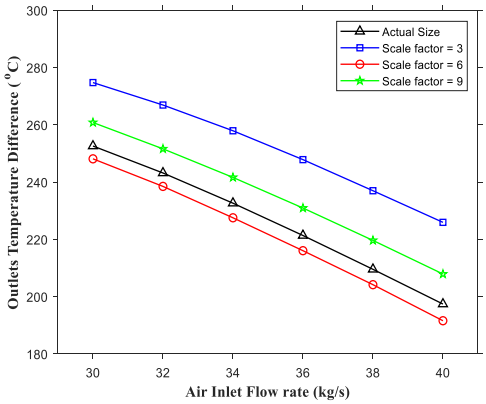

Figure 9 Variation of air inlet mass flow rate with clinker and air outlets temperature difference

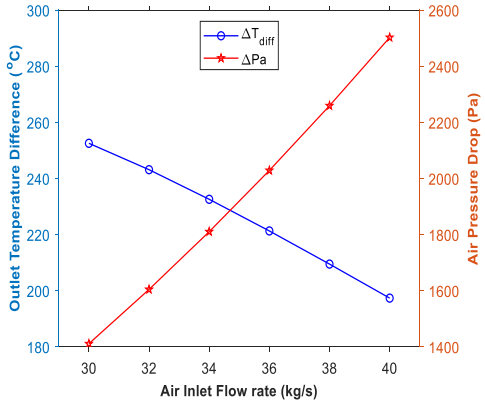

Figure 10 Variation of air inlet mass flow rate with clinker and air outlets temperature difference and pressure drop

3.4 Effects of clinker flow rate on clinker outlet temperature and air pressure drop

Performance of the clinker bed was also investigated by varying the mass flow rate of the clinker. Similarly, all other input parameters and geometrical parameters remain the same, while the clinker mass flow rate is varied from 60 kg/s to 85 kg/s at intervals of 5 kg/s. From Figure 11, it can be seen that as the clinker inlet flow rate increases, the clinker outlet temperature also increases. By comparing the performance for the three sizes of clinker bed, similar trend was observed as in the case where only the air inlet flow rate was varied. The clinker bed with scale factor 6 also predicted the maximum temperatures for each clinker flow rate, with the values closer to the actual size clinker bed. Clinker bed with scale factor 3, also produced minimum temperature values for each flow rate. In general, the minimum temperature 773.98℃ was estimated at flow rate 60 kg/s (i.e. actual size) for scale factor 3, while the maximum temperature 938.70℃ was estimated at flow rate 85 kg/s (i.e. actual size) for scale factor 6. The variation of clinker inlet mass flow rate with air outlet temperature is shown in Figure 12. From the figure, temperature of air at the outlet also increases with increase in clinker inlet flow rate. The bed with scale factor 3 produced higher temperatures, with the minimum and maximum values of 1087.8 ℃ and 1132.8 ℃ respectively, while the bed with scale factor 6 produced the lowest values at each clinker flow rate with the minimum and maximum values of 1067 ℃ and 1111.7 ℃ respectively. The difference between the temperature of clinker and air at their respective outlets after cooling was also observed and presented in Figure 13. The difference between the temperatures also decreases with increase in clinker flow rate. Figure 14 further shows the variation of clinker inlet flow rate with clinker and air outlets temperature difference and pressure drop for the actual size. The variation revealed that as the clinker flow rate increases, the temperature difference decreases, while the pressure drop remains constant.

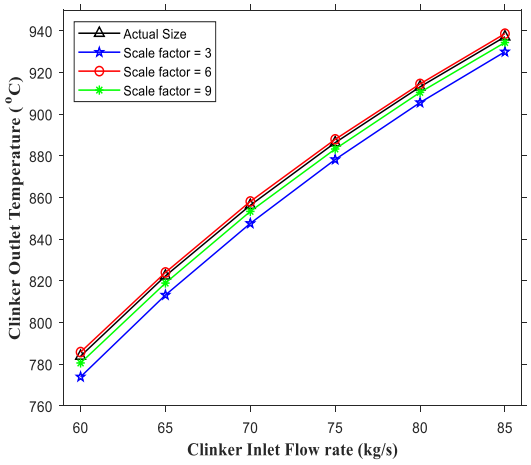

Figure 11 Variation of clinker inlet mass flow rate with clinker outlet temperature

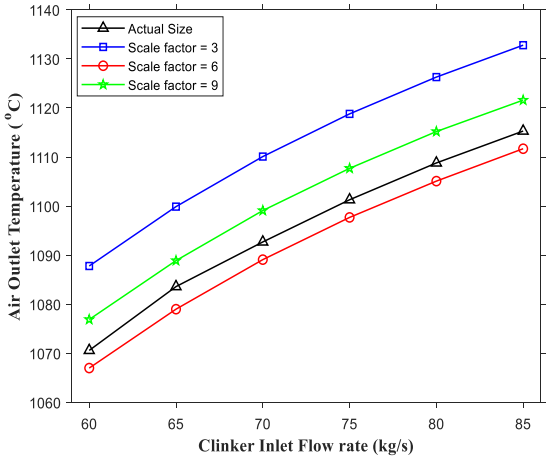

Figure 12 Variation of clinker inlet mass flow rate with air outlet temperature

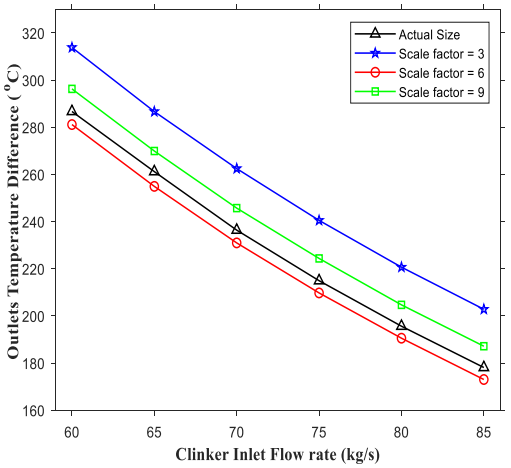

Figure 13 Variation of clinker inlet mass flow rate with clinker and air outlets temperature difference

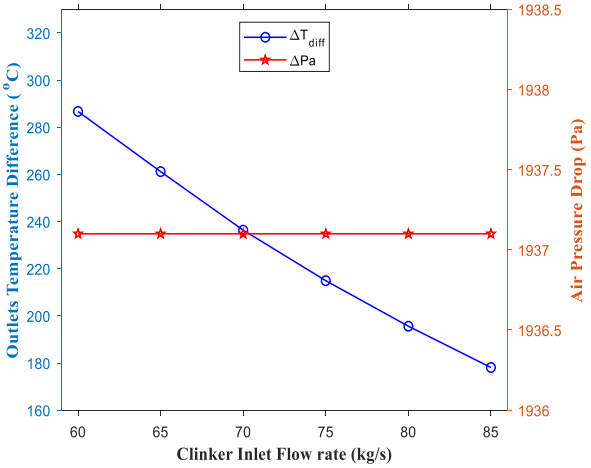

Figure 14 Variation of clinker inlet mass flow rate with clinker and air outlets temperature difference and pressure drop

3.5 Pumping power (P_p) and Thermal-Hydraulic Performance Factor (ϑ)

The pumping power is required to resist the drag in the porous domain of the clinker bed. This factor has been adopted by several researchers over the years in different heat transfer application [8, 35] and is estimated using equation (34). The thermal-hydraulic performance (TPF) number is a dimensionless parameter which establishes a balance between the rate of heat transfer enhancement and pressure drop [36, 37]. The thermal performance factor in porous media flow adopted by Moghadasi et al. [37], defined as a function of the pressure drop and Nusselt number ratio as follows was considered and presented as equation (36).

$$P_p = \Delta P_{air} \times \dot{V}_{air} \quad (34)$$

$$\dot{V}_{air} = \frac{\dot{m}_{air}}{\rho_{air}} \tag{35}$$

$$\varphi = \frac{Nu/Nu_b}{\Delta P/\Delta P_b} \tag{36}$$

where: where $\dot{V}$ is the volumetric flow rate of air (m^3/s), Nu is the Nusselt number estimated for the initial parameters of the clinker bed, Nu_b is the Nusselt number estimated when flow rate of air or clinker is varied, ΔP is the Pressure drop estimated for the initial parameters of the clinker bed (Pa) and ΔP_b is the Pressure drop estimated when flow rate of air or clinker is varied (Pa).

The estimated power consumption for variation of air mass flow rate is presented in Figure 15. The trend clearly shows that increase in mass flow rate of air will lead to increase in pumping power which consequently increases pumping cost. This trend was observed for all the sizes of clinker bed, but pumping power increases with reduction in size of clinker bed. The increase in pumping power with reduction in size of the clinker bed is attributed to the increase in pressure drop across the clinker bed as the size of the bed is reduced. Any of the small-scaled size could be used to study the exact temperature performance of the clinker bed which is expected to be obtained when an actual large size is used. For every pumping power of scaled down-size, the equivalent pumping power for the actual size can be obtained by diving it by its scale factor. The performances of all the four clinker bed geometries were compared in terms of thermal-hydraulic performance as shown in Figure 16.

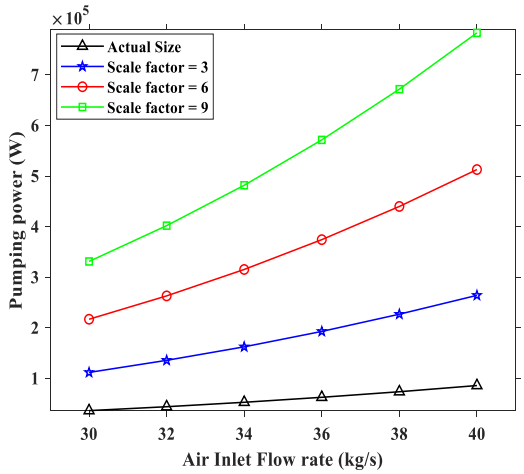

Figure 15 Variation of air inlet mass flow rate with Pumping power

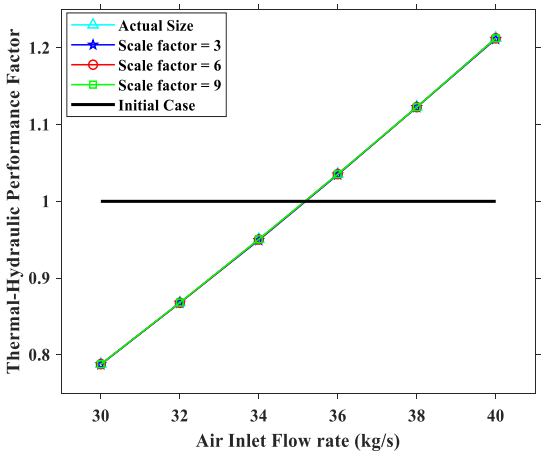

Figure 16 Variation of air inlet mass flow rate with TPF

It should be noted that the thermal-hydraulic performance of the initial parameters of clinker bed (i.e. $\dot{m}_{clk} = 72.32$ and $\dot{m}_{air} = 35.17$) was considered as the initial parameter used for validation, and its value is "1" being the reference value. For a process to be considered to yield improved performance ϑ must be greater than 1. These performances are applicable to all the clinker bed sizes considered, with negligible difference in the φ values estimated at each flow rate. However, ϑ values for scale factor 3 were the minimum for each flow rate, while the values for actual size were the maximum. The maximum percentage difference between the actual size and scaled size clinker bed (scale factor 3) ϑ was estimated to be 0.08% which indicates very close performance and is considered negligible. It was pointed out earlier that the smaller the size of the bed the larger the pressure drop estimated, the smaller sizes generally provide economical advantage because they help to achieve detailed investigation of the clinker bed, either through numerical simulation or development of small scale prototype at very little cost.

4. Conclusion

In this study, clinker cooler used in the cement plant for cooling down the temperature of hot clinker was considered for scaling down. Dimensional analysis using Buckingham Pi theorem was adopted and three scaled sizes with scale factor 3, 6 and 9 were obtained. Mathematical analysis was carried out for the actual size and the three scaled down-sizes. It was observed that the scaled sizes predicted similar results with negligible percentage difference. Findings from the study further revealed that predicted air outlet temperature when compared to the experimental and numerical solution result from literature yielded percentage deviations of –5.46% and +1.65% respectively. Considering the scaled down-sizes, predicted results when compared with the actual size experimental result, yielded negligible percentage deviation of 3.96%, 5.77% and 4.9% for scale factors 3, 6 and 9, respectively. The results further revealed that increase in the mass flow rate of air will improve the heat transfer performance of the clinker bed, but this comes with increase in pressure drop across the clinker bed height. In addition, increase in clinker flow rate was observed to be undesirable because the clinker outlet temperature, being expected to decrease also increased; however, the pressure drop remains unchanged. Additionally, the maximum percentage difference between the actual size and scaled sizes thermal-hydraulic performance factor ϑ, was 0.08% which indicates very close performance.

5. Acknowledgements

The authors acknowledge the expert support of Federal University of Technology Akure, Nigeria.

6. References

[1] Shao W, Chen X, Zhao T, Chen Q. Heat current model of solid granule cooling processes in moving packed beds and its applications. Chem Eng Res Des. 2020;156:384-90.

[2] John JP. Parametric studies of cement production processes. J Energy. 2020;2020:1-17.
[3] Hanein T, Glasser FP, Bannerman MN. Thermodynamics data for cement clinkering. Cem Concr Res. 2020;132:106043.
[4] Alsop PA. The cement plant operations handbook. 7th ed. Dorking: Tradeship Publications Ltd.; 2019.
[5] Cao Q, Zheng C, Sun Q, Cheng L. Numerical simulation of an improved structure for high-resistance grate plates. Energy Procedia. 2016;104:407-12.
[6] Okoji AI, Anozie AN, Omoleye JA, Osuolale FN. Thermodynamics and parametric study of the grate clinker cooler using the process model. IOP Conf. Ser: Mater Sci Eng. 2021;1107:012189.
[7] Shao W, Cui Z, Cheng L. Multi-objective optimization design of air distribution of grate cooler by entropy generation minimization and genetic algorithm. Appl Therm Eng. 2016;108:76-83.
[8] Shao W, Cui Z, Cheng L. Multi-objective optimization of cooling air distribution of grate cooler with different clinker particles diameters and air chambers by genetic algorithm. Appl Therm Eng. 2017;111:77-86.
[9] Cui Z, Shao W, Chen Z, Cheng L. Mathematical model and numerical solutions for the coupled gas–solid heat transfer process in moving packed beds. Appl Energy. 2017;206:1297-308.
[10] Shao W, Cui Z, Ma XT. Experimental research on cement grate cooler system and numerical simulation of its clinker cooling process. Appl Therm Eng. 2020;181:115904.
[11] Wang M, Liu B, Wen Y, Liu H. Numerical simulation and analytical characterization of heat transfer between cement clinker and air in grate cooler. J Chem Eng Jpn, 2016;49(1):10-5.
[12] Wang M, Liu B, Wen Y, Liu H. Seepage heat transfer between clinker and cooling air with variable properties in grate cooler. Heat Transf Res. 2017;48(3):263-81.
[13] Yao Y, Ding S, Chen Y. Modeling of the thermal efficiency of a whole cement clinker calcination system and its application on a 5000 MT/D production line. Energies. 2020;13(20):5257.
[14] Abdul W, Rößler C, Mawalala C, Pisch A, Hanein T, Bannerman M. Thermodynamic modeling of Portland cement clinkers. The 16th International Congress on the Chemistry of Cement 2023 (ICCC2023); 2023 Sep 18-22; Bangkok, Thailand. Bangkok: Thailand Concrete Association; 2023. p. 1-4.
[15] Okoji AI, Anozie AN, Omoleye JA. Evaluating the thermodynamic efficiency of the cement grate clinker cooler process using artificial neural networks and ANFIS. Ain Shams Eng J. 2022;13(5):101704.
[16] Kumar DS. Heat and mass transfer. 7th revised ed. New Delhi: S.K. Kataria & Sons; 2010.
[17] Coutinho CP, Baptista AJ, Rodrigues JD. Reduced scale models based on similitude theory: a review up to 2015. Eng Struct. 2016;119:81-94.
[18] Altun O, Wolniak P, Mozgova I, Lachmayer R. An analysis of scaling methods for structural components in the context of size effects and nonlinear phenomena. Proceedings of the Design Society: DESIGN Conference. 2020;1:797-806.
[19] Yoon J, Kim Y, Song H. Numerical and experimental analysis of thermal-flow characteristics in a pyrolysis reactor of a gas scrubber designed based on similitude theory. J Air Waste Manag Assoc. 2020;70(5):532-43.
[20] Douglas JF, Gasiorek JM, Swaffield JA, Jack LB. Fluid mechanics. 5th ed. Pearson Education Limited; 2005.
[21] Casaburo A, Petrone G, Franco F, Rosa SD. A review of similitude methods for structural engineering. Appl Mech Rev. 2019;71(3):1-32.
[22] Kenan H, Azeloğlu O. Design of scaled down model of a tower crane mast by using similitude theory. Eng Struct. 2020;220:110985.
[23] Zhang D, Gao P, Zhou Y, Wang Y, Zhou G. An experimental and numerical investigation on temperature profile of underground soil in the process of heat storage. Renew Energy. 2020;148:1-21.
[24] Zhou LL, Li DK. Design of scaled model for dynamic characteristics of stiffened cylindrical shells based on equivelent similar method. Aeronaut J. 2019;123(1261):398-415.
[25] Fallico C, Lauria A, Aristodemo F. Porous medium typology influence on the scaling laws of confined aquifer characteristic parameters. Water. 2020;12(4):1166.
[26] Oyepata JS, Akintunde MA, Dahunsi OA, Yaru SS, Idowu ET. Modelling of clinker cooler and evaluation of its performance in clinker cooling process for cement plants. Niger J Technol.2020;39(4):1093-9.
[27] Touil D, Belabed HF, Frances C, Belaadi S. Heat exchange modeling of a grate clinker cooler and entropy production analysis. Int J Heat Technol. 2005;23(1):61-8.
[28] Shao W, Cui Z, Liu Y. Multi-objective optimization on clinker layer thickness of a grate cooler based on entropy generation. Energy Procedia. 2019;158:5811-6.
[29] Ma X, Cao Q, Cui Z. Optimization design of the grate cooler based on the power flow method and genetic algorithms. J Therm Sci. 2020;29:1617-26.
[30] Shao W, Cui Z, Cheng L. Multi-objective optimization of cooling air distributions of grate cooler with different inlet temperatures by using genetic algorithm. Sci China Technol Sci. 2017;60:345-54.
[31] Yin HC, Zhu YS, Li DF. Numerical simulation and research of grate cooler based on coupled gas-solid heat transfer. J Therm Sci Technol. 2012;3:229-33.
[32] Liu B, Wang M, Wen Y, Hao X, Fan X. Research on control mechanism model of grate cooler based on seepage heat transfer theory. J Comput Inf Syst. 2013;9(20):8281-8.
[33] Poling BE, Prausnitz JM, O'Connell JP. The properties of gases and liquids. 5th ed. New York: McGraw – Hill; 2020.
[34] Batul B, Sohail A, Aizaz A, Jamil Z. Application of structural similitude for scaling of a pressure vessel. IOP Conf Ser: Mater Sci Eng. 2019;642:012004.
[35] Chen K, Wu W, Yuan F, Chen L, Wang S. Cooling efficiency improvement of air-cooled battery thermal management system through designing the flow pattern. Energy. 2019;167:781-90.
[36] Mogaji TS, Olapojoye AO, Idowu ET, Saleh B. CFD study of heat transfer augmentation and fluid flow characteristics of turbulent flow inside helically grooved tubes. J Braz Soc Mech Sci Eng. 2022;44:90.
[37] Moghadasi H, Bayat M, Aminian E, Hattel JH, Bodaghi M. Computational fluid dynamics study of laminar forced convection improvement of a non-newtonian hybrid nanofluid within an annular pipe in porous media. Energies. 2022;15(21):8207.